doi: 10.1016/S0022-2836(02)00198-5 available online at http://www.idealibrary.com on IDEAL® J. Mol. Biol. (2002) 318, 1307–1316

JMB

Crystal Structure of a Non-canonical High Affinity Peptide Complexed with MHC Class I: A Novel Use of Alternative Anchors

Vasso Apostolopoulos[1,2*†], Minmin Yu[1†], Adam L. Corper[1], Wenjun Li[1] Ian F.C. McKenzie[1], Luc Teyton[3] and Ian A. Wilson[1*]

[1]*Department of Molecular Biology BCC-206 and Skaggs Institute for Chemical Biology The Scripps Research Institute 10550 North Torrey Pines Road La Jolla, CA 92037, USA*

[2]*Immunology and Vaccine Laboratory, The Austin Research Institute Studley Road, Heidelberg Vic. 3084, Australia*

[3]*Department of Immunology The Scripps Research Institute 10550 North Torrey Pines Road La Jolla, CA 92037, USA*

**Corresponding authors*

The crystal structure of a non-standard peptide, YEA9, in complex with H-2K^b, at 1.5 Å resolution demonstrates how YEA9 peptide can bind with surprisingly high affinity through insertion of alternative, long, non-canonical anchors into the B and E pockets. The use of "alternative pockets" represents a new mode of high affinity peptide binding, that should be considered when predicting peptide epitopes for MHC class I. These novel interactions encountered in this non-canonical high affinity peptide–MHC complex should help predict additional binding peptides from primary protein sequences and aid in the design of alternative approaches for peptide-based vaccines.

Keywords: MHC class I; non-canonical anchor motif peptides; YEA9; vaccine design; H-2K^b

Introduction

The MHC class I consists of a polymorphic transmembrane heavy chain which is non-covalently associated with β2-microglobulin. In 1987, the first X-ray crystallographic structure of an MHC class I molecule, HLA-A2, demonstrated that the α1 and α2 domains combine to form a platform of eight antiparallel β strands that were straddled by two long antiparallel α helices.[1] A groove is formed between the helices that identified the binding site for peptide antigens. Later, when single peptide complexes for human and murine MHC class I were determined,[2–5] the side-chains of certain peptides, called anchor residues,[6,7] were shown to fit into specificity pockets on the floor of the groove. The amino acid residues that line the peptide-binding groove determine the individual specificity of the peptide–MHC interaction. The peptide binding groove can be subdivided into various pockets (A–F),[8] that are linked by polymorphic residues that define each MHC allele. The non-anchor peptide residues that point upwards usually interact with the TCR.

For H-2K^b, anchors are in positions P6 and P9 for 9-mers or P5 and P8 for 8-mers, with preferred anchors of Phe/Tyr-P5 or P6 and Leu at P8 or P9. Tyr-P3 in some situations is also preferred. These anchor residues are usually required for stabilization and high-affinity binding of peptide to MHC; however, peptides which do not contain the canonical anchor residues can still bind and be presented by MHC class I and be targets for (cytotoxic T lymphocytes (CTL).[9–16] It is not clear how non-standard peptides are presented by MHC class I molecules. We previously noted a peptide lacking canonical anchor motifs (YEA9; SRDHSRTPM), derived from yeast, binds to H-2K^b molecules.[17] Thus, we determined the crystal structure of YEA9, at high resolution (1.5 Å), bound to murine MHC class I, H-2K^b. The YEA9 complex has given unexpected insights into how high-affinity peptide binding can be achieved by the use of alternative residues that insert into non-canonical specificity pockets.

† These authors contributed equally to this work.
Abbreviation used: MPD, 2-methyl-2,4-pentanediol.
E-mail addresses of the corresponding authors: v.apostolopoulos@ari.unimelb.edu.au; wilson@scripps.edu

0022-2836/02/$ - see front matter

Table 1. Comparison of 8 and 9-mer peptides binding to H-2K^b

Peptide sequence	Source	Reference
1 2 3 4 5 6 7 8 9		
S R D H S R T P M	Yeast (YEA9)	17
S A P D T R P A P	MUC1 VNTR (MUC1-9)	12
R F H N I R G R W	E6, HPV type 16	16
V A P V R L I L L	Peptide eluted from H-2K^{bw9}	26
V E P V R L I L L	Peptide eluted from H-2K^{bw9}	26
V A P E E H P T L	Peptide eluted from H-2K^{bw9}	26
F A P G N Y P A L	Sendai virus NP$_{324-332}$ (SEV9)	41
Y S G Y I F R D L	Rotavirus VP3$_{585-593}$	42
1 2 3 4 5 6 7 8		
S I I N F E K L	Chicken ovalbumin$_{257-264}$ (OVA8)	43
R G Y V Y Q G L	Vesicular stomatitis virus NP$_{52-59}$ (VSV8)	44
S I Y R Y Y G L	Synthetic strong agonist for 2C TCR (SIYR)	45
E Q Y K F Y S V	Self agonist for 2C TCR (dEV8)	46
R G Y V Y Q E L	Antagonist for 2C TCR (EVSV)	46
L S P F P F D L	Weak agonist for 2C TCR (p2Ca)	47
S A P D T R P A	MUC1 VNTR (MUC1-8)	12

Amino acids highlighted in red are the standard anchor motifs for peptide binding to H-2K^b molecules.[6] Amino acids highlighted in green are non-standard side-chains found in peptides associated with H-2K^b molecules. The one-letter code for the amino acids is used. The 9-mer peptides are shown on top, followed by 8-mer peptides. In H-2K^b, the longer 9-mer peptides bulge out between P4 and P6 but the positions of their ends are conserved; hence, the gap introduced between P4 and P5 for 8-mer peptides is to maintain similar alignment in 8-mer and 9-mer peptides. The crystal structures of SEV9,[5] OVA8,[17] VSV8,[5] SIYR,[21] dEV8[21] and MUC1-8 (accompanying paper)[15] peptide complexes are known.

Results

Identification of a non-canonical peptide binding to MHC class I, H-2K^b, and affinity measurements

During the expression of MHC class I molecules in *Drosophila melanogaster* cells, yeast peptides (yeastolate) are added by the manufacturers to the culture medium and subsequently bind to H-2K^b and to other MHC molecules when the proteins are expressed in that medium.[17] One of these peptides fortuitously stabilizes H-2K^b and facilitates its purification.[18] Fortunately, very high affinity peptides added after purification displace these yeast peptides[17,19] and permit purification, crystallization and structure determination of single peptide complexes with H-2K^b.[5,17,20,21] The predominant peptide found in the peptide-binding groove of purified soluble H-2K^b molecules has been identified as a yeast 9-mer peptide (SRDHSRTPM; YEA9) (Table 1). This peptide, which derives from the yeast α-glucosidase protein, residues 438–446 (maltase), contains a large polar Arg residue at P6 rather than the preferred aromatic Phe or Tyr, similar to the tumor-associated E6 human papillomavirus type-16 protein (RFHNIRGRW)[16] and the low-affinity MUC1-9 peptide isolated from human Mucin 1, SAPDTRPAP, a tumor-associated antigen (Table 1).[21,22] YEA9 also contains large P2 (Arg) and P9 (Met) residues that could possibly act as effective anchors.

We determined the crystal structure of the high-affinity non-canonical anchor motif peptide YEA9 in complex with H-2K^b and compared it to the high-affinity canonical anchor motif peptide, SEV9. The YEA9 peptide, which does not contain any canonical anchors at P2, P3, P5/6, but does have large side-chains at these positions, has relatively high affinity for H-2K^b in the 10^{-8}M range (Table 2). Mutation of Ser-P1 to Ala does not alter the affinity of the peptide binding to H-2K^b at 23 °C, but reduces its stability by 20-fold at 37 °C (Table 2). Mutation of Arg-P2 to Ala slightly reduces the affinity, whereas, mutation of Arg-P6 to Ala destabilizes the complex at 37 °C by about tenfold. The double Ala mutations at P2 and P6 have an even more pronounced effect, especially at 37 °C (Table 2). Substitutions at P2 and P6 indicate these two residues together play a significant role in peptide binding. Mutation of P3-Asp to Ala reduces the affinity and stability of the peptide substantially, indicating that P3-Asp plays a major role in peptide binding. Mutation

Table 2. Affinity measurements of YEA9 peptides binding to H-2K^b

Peptide	Sequence	4 °C K_D (nM)	23 °C K_D (nM)	37 °C K_D (nM)	H-bonds (side-chain of peptide with MHC)
YEA9	SRDHSRTPM	190	90	140	
YEA9(1A)	**A**RDHSRTPM	730	86	2700	P1-Lys66 and Glu63
YEA9(2A)	S**A**DHSRTPM	180	69	190	P2-Glu24
YEA9(3A)	SR**A**HSRTPM	630	3100	3500	P3-Arg155
YEA9(4A)	SRD**A**SRTPM	220	64	360	
YEA9(5A)	SRDH**A**RTPM	200	40	330	
YEA9(6A)	SRDHS**A**TPM	140	120	1300	P6-Asp77
YEA9(7A)	SRDHSR**A**PM	380	51	320	P7-Glu152
YEA9(8A)	SRDHSRT**A**M	330	38	330	
YEA9(9A)	SRDHSRTP**A**	130	3000	3800	
YEA9(2A6A)	S**A**DHS**A**TPM	220	355	25000	
SEV9	FAPGNYPAL	5	3	30	
OVA8	SIINFEKL	6	10	82	
VSV8	RGYVYQGL	34	27	163	

The affinity values in this Table are the mean of five values. The standard errors of these values are between 10-15%.

of P9-Met to Ala also significantly decreased the affinity and stability of the peptide. Mutations of amino acid residues at positions P4, P5, P7 and P8 had little effect on the affinity of the peptide. Thus, these Ala substitutions indicate that positions P2, P3, P6 and P9 play a major role in peptide affinity and stabilization.

Structure and interactions of the non-canonical YEA9 peptide with H-2K^b

The crystal structure of H-2K^b-YEA9 at 1.5 Å resolution was determined by molecular replacement to an R_{free} value of 22.2% (Table 3). The final model consisted of H-2K^b heavy chain, α1-274, β_2 microglobulin, β1-99, four carbohydrate moieties (three at Asnα176 and one at Asnα86) and all peptide residues. The electron density for the bound peptide was continuous and well resolved, except for the side-chain density of Arg-P6 (Figure 1(a) and (b)). Furthermore, the *B*-value for Arg-P6 was high, which is unusual for side-chains corresponding to primary anchor positions. Superposition of the β-sheet floor of the H-2K^b α1/α2 domain of YEA9 and SEV9 complexes gave average root-mean-square deviations (rmsd) for the peptide C^α positions of 0.97 Å (P1–P4) and 1.58 Å (P5–P9), although they retain significant similarity at their N and C termini. An upward bulge between P5 and P7 (2.5 Å, maximum at P6 C^α) arises in the YEA9 peptide through non-optimal fit of the Arg-P6 in the C pocket, and thus, makes use of the alternative E pocket (Figure 1(c) and (d)). Such large peptide bulges in murine class I

Table 3. Data processing and refinement statistics

A. Data processing and refinement	
Cell dimensions (Å)	$a = 136.1$, $b = 88.3$, $c = 45.7$
R_{sym} (%)[a]	3.5 (46.7)[b]
Resolution range (Å)	50.0–1.5 Å
Unique reflections	82,816 (3649)
Data redundancy	3.5 (2.8)
Data completeness (%)	92.9 (82.3)
$\langle I/\sigma \rangle$	33.7 (2.1)
R_{cryst} (%)[c]	20.6
R_{free} (%)[d]	22.2
Bond length rms deviation (Å)	0.005
Bond angle rms deviation (°)	1.27
Average *B* values (Å^2) (protein (peptide))	24 (29)
No. water molecules (average *B* in Å^2)	281 (32)
B. Ramachandran plot analysis[e]	
Residues in most favored regions (%)	92.1
Residues in additional allowed regions (%)	7.3
Residues in generously allowed regions (%)	0.6
Residues in disallowed regions (%)	0.0

[a] $R_{sym} = 100[\sum_h \sum_i |I_i(h) - \langle I(h) \rangle| / \sum_h \sum_i I_i(h)]$, where $I_i(h)$ is the *i*th measurement of the *h* reflection and $\langle I(h) \rangle$ is the average value of the reflection's intensity.

[b] Data for the highest-resolution shell, 1.53–1.50 Å.

[c] $R_{cryst} = \sum ||F_o| - |F_c|| / \sum |F_o|$, where F_o and F_c are the observed and calculated structure factor amplitudes within the set of reflections used for refinement.

[d] $R_{free} = \sum ||F_o| - |F_c|| / \sum |F_o|$, was calculated for a randomly selected set of structure factors (~10%) and not used in refinement.

[e] The Ramachandran plot was generated using PROCHECK.[39]

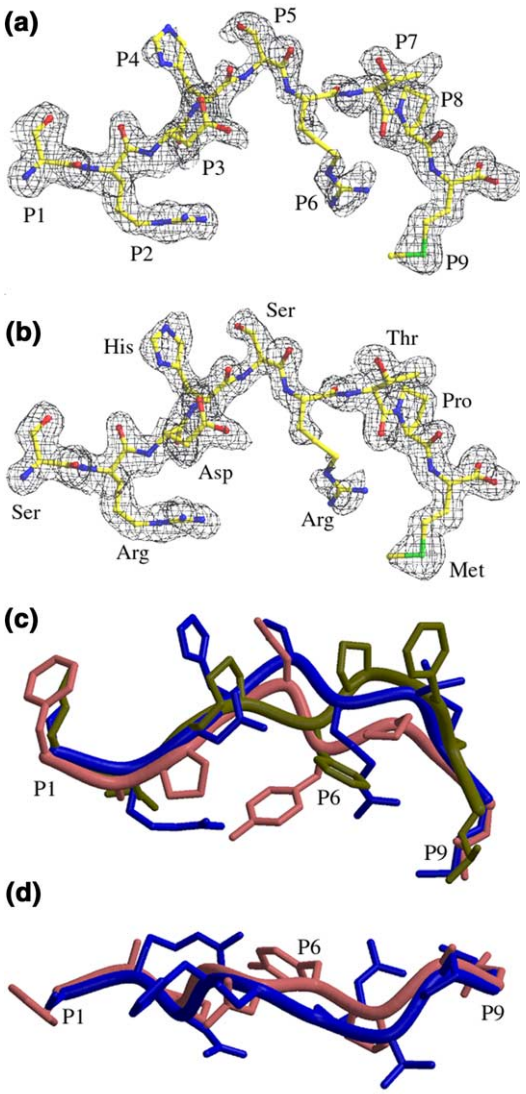

Figure 1. Peptide density and conformations when bound to H-2K^b. Electron density of YEA9 peptide in the H-2K^b binding groove: (a) initial $F_o - F_c$ map contoured at 1.5σ prior to any peptide fitting and (b) final σ_A-weighted $2F_o - F_c$ map contoured at 1.0σ for the refined structure at 1.5 Å. Comparison of 9-mer peptides: (c) side view, (d) top view. For comparison, a side view of QL9 peptide modelled from a bound 9-mer complexed with H-2L^d is shown in (c). H-2K^b residues in the various complexes were superimposed only on their β-sheet floors and the resulting peptide overlaps were produced. The peptide conformations represent their structures in the H-2K^b bound form. The Figure was drawn using programs MOLSCRIPT and Raster3D. Peptide colors are as follows: YEA9, dark blue; SEV9, salmon; H-2L^d QL9, olive.

complexes have been noted for H-2D^b and H-2L^d, but are normally caused by peptides having to circumvent prominent ridges that arise from large hydrophobic MHC residues on the floor of the binding groove,[23–25] which are not present in H-2K^b (Figure 1(c)). A large backbone sidewards deviation (~1.0 Å), around P6–P7, is also observed for YEA9 towards the α2 helix (Figure 1(d)).

The YEA9 peptide complex contains all of the main-chain hydrogen bonds present in OVA8, VSV8 and SEV9 peptide complexes,[2,5,17] as well as some additional ones. A unique hydrogen bond in YEA9 is found between Gluα152 O$^{\varepsilon 1}$ and the amide nitrogen at Thr-P7, as a result of the peptide bulge; similarly a novel hydrogen bond is formed between the backbone of Thr-P7 and Gluα152 (Figure 2(a)). Furthermore, novel hydrogen bond interactions between the side-chains Asp-P3 and Arg-155 help anchor YEA9. In addition, Arg-P2 forms a buried salt-bridge with Gluα24 O$^{\varepsilon 2}$ in the B pocket (Figure 2(b)). It appears then that Arg-P2 in YEA9 can act as a substitute anchor and, consequently, does not allow Arg-P6 to occupy the C pocket due to steric hindrance and charge repulsion (Figures 2 and 3). A similar situation has been described, but in this case for an MHC class I mutant H-2K^{bw9}, in which Valα9 of the MHC was replaced by Trp in order to eliminate the C pocket. This mutation drastically altered the peptide selection to exclusively 9-mer peptides, where Pro-P3 and Arg-P5 were predominantly selected as new primary anchors.[26] It was proposed that Arg-P5 would most likely contact the E pocket with possible salt-bridge and hydrogen bond interactions with Aspα77, Tyrα116 and Gluα152. It is interesting to note that a similar arrangement of Pro-P3 and Arg-P6 residues could act as anchors for MUC1-9. In YEA9, NH1 and NH2 of Arg-P6 do indeed form hydrogen bonds with Aspα77 O$^{\delta 2}$ (Figure 2(a)) and from our peptide mutation studies and affinity measurements, Arg-P6 plays a role in the stability of the peptide at 37 °C which is enhanced further with the interactions of Arg-P2. The human papillomavirus type 16, E6 peptide has a large non-polar Phe at P2 and positively charged residues His-P3 and Arg-P6 (Table 1). Presumably, the charge repulsion at P3 or the large P2 residue would repel Arg-P6 from the C pocket in favor of binding to the E pocket. In MUC1-9, Arg-P6 could presumably bind in a similar way to the E pocket rather than the C pocket, causing a bulge at P7–P9 residues that would render the C terminus more accessible, consistent with the observed interactions of this peptide complex with anti-peptide antibodies.[22]

The stability and the affinity of peptides is dependent on optimally filling the pockets in the core of the binding groove, and specific anchor residues are usually necessary for optimal stability.[8,19] The OVA8 structure has large hydrophobic residues of Ile-P2 and Phe-P5, which allow a tight packing in the P2–P5 (C) pocket. VSV8 and SEV9 have a large side-chain at Tyr-P5/6 in the C pocket and a large secondary anchor of Tyr and Pro at P3, respectively; thus, the gap between the B and C pockets is minimized. Comparison of the relative filling or occupancy of the H-2K^b B and C

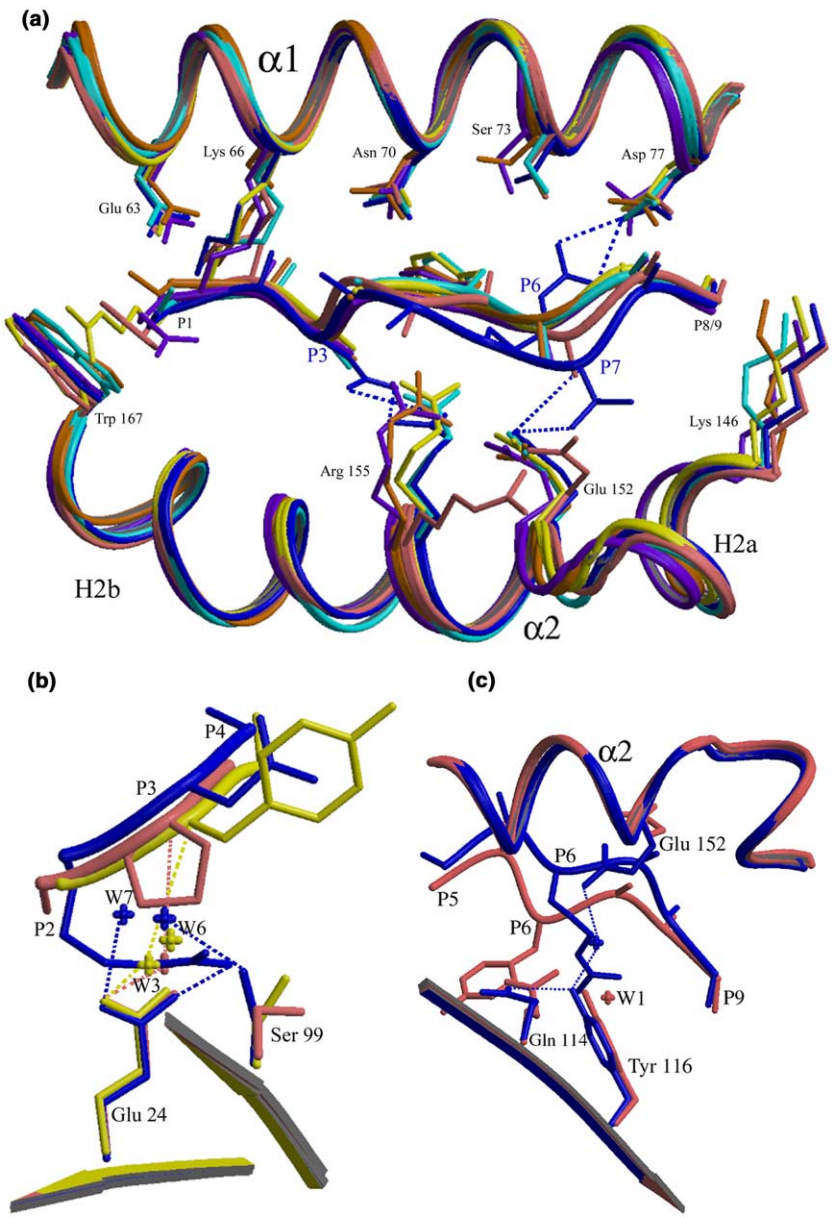

Figure 2. Comparison of the peptide binding grooves in the H-2K^b crystal structures. (a) Six structures were overlapped by superimposition of the β-sheet floor. The α1α2 helices superimpose closely, with some side-chain variations at Lysα66, Asnα70, Serα73, Aspα77, Lysα146, Gluα152, Argα155 and Trpα167. Peptides are shown as a C$^\alpha$C$^\beta$ trace, except for P1, P5/6 (all peptides), as well as P3, P6 and P7 of the YEA9 peptide. Novel hydrogen bonds not present in other structures are shown for YEA9 (blue). (b) Side view of YEA9 (blue), SEV9 (salmon) and VSV8 (yellow) peptides showing P2 and P3 side-chains and P4 C$^\alpha$C$^\beta$. Hydrogen bonds and water molecules in YEA9 are shown that are not present in other H-2K^b structures as well as the side-chain rotamer differences for Serα99. (c) Side view of YEA9 and SEV9 peptides showing the P6 side-chain and P5, P7, P8, P9 C$^\alpha$C$^\beta$. Novel hydrogen bond interactions for YEA9, not present in SEV9, are shown in blue. The Figure was generated using programs MOLSCRIPT and Raster3D. Peptide colors are as follows: OVA8, turquoise; VSV8, yellow; YEA9, dark blue; SEV9, salmon; dEV8, purple; SIYR, orange.

specificity pockets by YEA9 and SEV9 (Figure 3(a)–(c)), OVA8, VSV8 (see Figure 4(a) and (b) of Apostolopoulos *et al.*, the accompanying paper[15]) reveals major differences. As a consequence of Arg-P6 in YEA9 not occupying the C pocket, but instead pointing towards the E pocket, a conserved water molecule W1, as well as W4 and W5 (Figures 2 and 3) are displaced between P6/P7 and the side-chain of Tyrα116. As a result, the aromatic side-chain of Tyrα116 is shifted 1.05 Å (hydroxyl to hydroxyl) compared to SEV9 to form another novel hydrogen bond to Glnα114 and a water-mediated hydrogen bond to Gluα152 (Figure 2(c)), analogous to the shifts seen for Tyrα116 in HLA-A2.[27] W2 is present in YEA9 as in SEV9, while W3 is displaced by Arg-P2 in YEA9 (Figures 2(b) and 3(a)–(c)) and W6 hydrogen bonds to Serα99 (Figure 2(b)). In addition, YEA9 has a unique water molecule, W7, which hydrogen bonds to Gluα24 and Asnα70 (Figures 2(b) and 3(a)).

In summary, the non-canonical peptide YEA9 can still bind to MHC class I with relatively high affinity despite non-occupancy of the central C pocket; the B and E pockets now become the principal side-chain anchoring positions. Large side-chains at P2, P6 and P9, and novel salt-bridge or hydrogen bonds to P2, P3, P6 and P7 residues contribute to anchoring the peptide in the MHC groove. Thus, we outline here the first structural description of a new mode for high-affinity peptide binding that should be invaluable in the identification and prediction of new peptide ligands for MHC class I molecules.

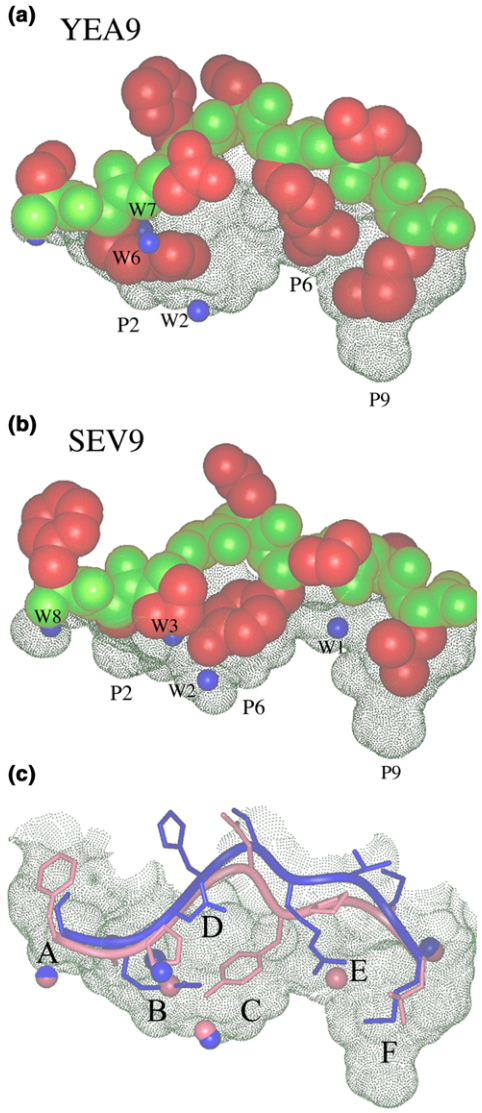

Figure 3. Comparison of occupancy of specificity pockets in different H-2K^b structures. (a) and (b) The 9-mer peptides YEA9 and SEV9. For comparison to 8-mer peptides OVA8 and VSV8, refer to the accompanying paper.[15] Molecular surfaces for the MHC binding groove (dotted surface) were calculated with a probe radius of 1.4 Å with Insight II (Biosym Technologies, San Diego CA, USA). The peptides are in CPK space-filling representation (backbone, green; side-chains, red) and labelled P1–P9 or P1–P8. (c) P2 occupies the B pocket, P5/6 the C pocket and P8/9 the F pocket. Water molecules (W) rendered as spheres of one-half van der Waals radii are colored blue.

Cavities and side-chain flexibility in the central C pocket

Internal cavities have been associated with increased conformational flexibility and multiple side-chain conformations for a single protein.[28] A large cavity appears precisely at the C pocket (P6) in YEA9 (111 Å^3), but not in SEV9, OVA8 or VSV8 (Figure 4). Even though a large cavity is present in the central C pocket, this does not substantially decrease the affinity of the peptide. In this situation, P2 and P6 (and hydrogen bonds at P3 and P7) must play a role in restoring the affinity and stability of the peptide complex. A small cavity (14–26 Å^3) is present in the F pocket for all complexes (Figure 4). VSV8 and SEV9 have in addition only a very small cavity (16 Å^3 and 39 Å^3, respectively) at the B pocket, whereas OVA8 is almost a perfect fit for all buried pockets other than F. Furthermore, the *B*-value (measurement of the average displacement of an atom due to thermal motion, conformational disorder, and static lattice disorder) of Arg-P6 in YEA9 is high (55 Å^2), which indicates that there is non-optimal local fit, and possible flexibility in this pocket. The *B*-values are low (9–25 Å^2) for side-chains pointing into the MHC groove for SEV9 (P2/6/9), YEA9 (P2/9) and OVA, VSV8 (P2/5/8), suggestive of a tight fit (Figure 4). High *B*-values are found for the upwards pointing residues of all peptides (>40 Å^2) (Figure 4).

Optimal peptide binding to H-2K^b is critically dependent upon filling the C pocket, which is not the case with YEA9. The large cavity present in YEA9 can be compensated by a large anchor Arg-P2, which restores some of the lost peptide–MHC interactions, as well as forming a buried salt-bridge. Importantly, the displaced Arg-P6 then finds another specificity pocket (E) with which to interact and forms a novel hydrogen bond and salt-bridge with Aspα77, which presumably helps stabilize the peptide in the groove. In addition the hydrogen bond between Asp-P3 and Argα155 plays a major role in peptide affinity and stability. Thus, Asp-P3 and both Arg-P2 and Arg-P6, contribute significantly to the thermal stability of the YEA9 peptide.

Discussion

The crystal structures of high-affinity, canonical anchor motif peptides binding to murine MHC class I H-2K^b, have been previously described for 9-mer SEV9 and 8-mers, VSV8, OVA8, dEV8 and SIYR peptides (Table 1 and Figure 2).[5,17,20,21] These peptides bind in a canonical manner making use of the B, C (D) and F pockets with preferential amino acid residues of Phe/Tyr-C pocket and the Leu-F pocket. However, until now little structural information has been available on the binding of non-standard peptides (peptides not containing either Phe/Tyr at P5 or P6 and Leu at P8 or P9) to MHC class I, and whether they differ in their interaction with the MHC molecule and, hence, with the T-cell receptor. It is now clear from a number of studies that non-canonical anchor motif-containing 8–9-mer peptides can bind to MHC class I and be targets for cytotoxic T-cells.[9–16] We have, therefore, determined the crystal structure of a peptide lacking the canonical Phe/Tyr-P6 and Leu-P9 anchors, YEA9 (SRDHSRTPM), in complex

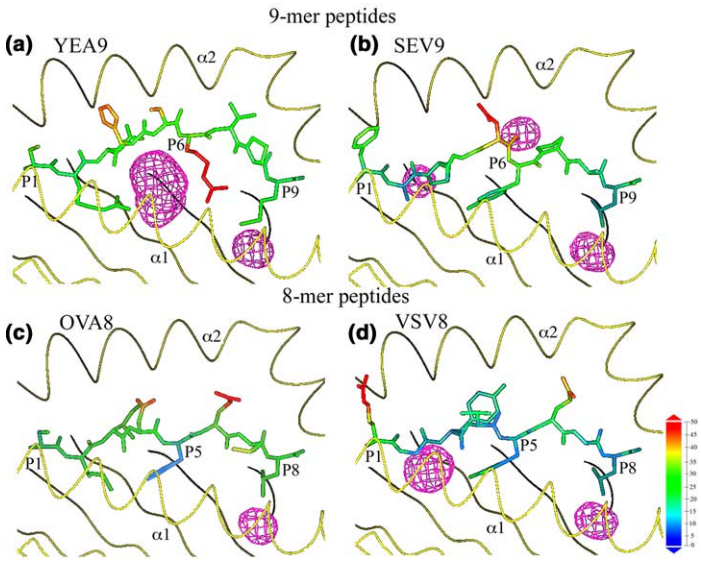

Figure 4. Internal cavities formed between the peptide and H-2K^b. (a) and (b) The 9-mer peptides YEA9 and SEV9 and compared to (c) and (d) 8-mer peptides OVA8 and VSV8. The peptide trace is represented by the *B*-values (blue ~5 Å^2 to red ~45 Å^2; *B*-value scale bottom right) and oriented from P1–P8/9. The Figure was generated with Insight II. Internal cavities (pink mesh) were calculated using the program SURFNET[48] in the presence of bound water molecules. A large internal cavity is found in the non-canonical peptide complex, YEA9, compared to the standard high-affinity peptide complexes (SEV9, OVA8 and VSV8).

with MHC class I H-2K^b, and compared its mode of binding to peptides that contain the canonical anchor motifs (Table 1 and Figures 1–4, 9-mer, SEV9 and 8-mers OVA8 and VSV8). We have also determined the crystal structure of another non-canonical anchor motif peptide, which binds with low affinity, and this is demonstrated in the accompanying paper.[15]

The non-canonical anchor motif peptide, YEA9, binds with relatively high affinity (10^{-8} M range) by insertion of long non-canonical anchor residues into the B and E pockets (Figure 3). Due to charge repulsion and steric hindrance, Arg-P2 in the B pocket prevents Arg-P6 from occupying the C pocket, causing a prominent bulge between P5 and P7; as a consequence, Arg-P6 points into the E pocket displacing a conserved water molecule (Figure 3). As a result of Arg-P6 now occupying the E pocket, the C pocket is left vacant, forming a large cavity, that is not found in the other high-affinity peptide-H-2K^b complexes (Figure 4). In addition, Arg-P6 has a very high *B*-value, indicating flexibility within this region. Despite this different anchor interaction, YEA9 binds with relatively high affinity and is stable at 37 °C. Arg-P2 forms a novel buried salt-bridge with Gluα24 and novel hydrogen bonds are formed between Asp-P3/Argα155, Arg-P6/Aspα77 and Thr-P7/Gluα152, all of which help anchor YEA9 in the groove, in addition to Met-P9. It would be expected that formation of such a large buried cavity would allow additional water molecules to enter and would help fill the non-optimally substituted pockets. YEA9 does not have any additional water molecules in the C pocket, but has a novel water molecule (W7) in the B pocket that hydrogen bonds to the MHC molecule. The absence of "rescuing" water molecules to bridge peptide and MHC[29] would contribute to a lower stability and affinity of the peptide. Rescuing water molecules have also been noted with the glycopeptide K2G in complex with H-2D^b, which does not have the canonical Asn-P5 anchor, but Ser-O-GlcNAc, and, as a consequence, the glycosylated side-chain points upward away from the peptide binding groove.[30] This leaves the C pocket empty; however, two water molecules help fill the pocket and hydrogen bond to the side-chains of the MHC.[30]

There is great interest in using synthetic peptides for peptide-based vaccine design. Motifs or canonical amino acid anchor residues have been the main focus for identifying peptide epitopes within a protein sequence. Here, we demonstrated the crystal structure of a relatively high-affinity peptide, binding to MHC class I H-2K^b, which does not contain the canonical Phe/Tyr-P6 but Arg-P6. It is now clear that peptides lacking canonical anchor motifs can also bind to MHC class I with relatively high affinity, and that alternate P2, P6 and P9 residues can contribute in anchoring the peptide into the peptide-binding groove in a different way to standard canonical peptides.[5,17,21] These studies are important as they show that binding of peptide with high affinity can occur in two ways: (i) by canonical hydrophobic anchors binding in the C and F pockets; and (ii) by non-canonical anchors binding in the B, E and F pockets. This study represents the first demonstration of the use of "alternative anchors" that differs from the published canonical preferences.[5–7,17,21] We propose that sequences that contain xRDxxRxxM/L should be taken into consideration when predicting potential T-cell epitopes for H-2K^b from a protein sequence. Non-canonical anchor motif peptides could be of value in immunotherapy studies; these new insights into the unexpected diversity of peptides that can bind to an MHC molecule holds promise for design of alternative peptide immunogens against many diseases.

Materials and Methods

Peptides

SRDHSRTPM, yeast (YEA9); SADHSRTPM, (YEA9-2A); SRAHSRTPM, (YEA9-3A); SRDASRTPM, (YEA9-4A); SRDHARTPM, (YEA9-5A); SRDHSATPM, (YEA9-6A); SRDHSRAPM, (YEA9-7A); SRDHSRTAM, (YEA9-8A); SRDHSRTPA, (YEA9-9A); SADHSATPM, (YEA9-2A6A); FAPGNYPAL, Sendai virus $NP_{324-332}$ (SEV9); SIINFEKL, chicken ovalbumin$_{257-264}$ (OVA8); RGYVYQGL, vesicular stomatitis virus NP_{52-59} (VSV8), were synthesized at the Austin Research Institute, using an Applied Biosystems model 430A machine. The purity of the peptides (>95%) was determined by mass spectrometry.

Affinity measurements of peptides bound to H-2K^b molecules

Affinity measurements for binding of peptides to soluble K^b molecules were performed as described.[19,31] Briefly, VSV8 peptide was labelled with ^{125}I (Amersham Pharmacia Biotech, Buckinghamshire, UK) using the Iodogen method. The [^{125}I]VSV8 peptide was purified using a Sep-Pak column (Waters, Milford, MA). The specific activity of the peptide was 26,636 cpm/ng. The competition assays were performed at 4 °C, 23 °C and at 37 °C as described[31] with a few modifications. The binding studies were carried out in 1% (v/v) fetal calf serum (FCS) and the free peptide was removed by gel filtration on Sephadex columns (NAP-5; Amersham Pharmacia Biotech). The dissociation constants for unlabelled peptides were determined from the molar concentrations of unlabelled peptides that gave 50% inhibition of [^{125}I]VSV8 binding to K^b molecules.

Preparation and crystallization of H-2K^b/YEA9 complex

The soluble extracellular domains of H-2K^b (heavy chain residues α1–274 and β_2-microglobulin residues β1–99) were expressed in *D. melanogaster* cells, as described.[5,18,19,32] The peptide SRDHSRTPM (YEA9) is already present in the binding groove of "empty" H-2K^b from the maltase "yeastolate" mixture present in Schneider's medium.[17] Large single crystals of the H-2K^b–YEA9 complex were grown in 1.8 M NaH_2PO_4/K_2HPO_4 with 2% (w/v) MPD (pH 7.25) at 22.5 °C with no addition of any other peptide.

Data collection and structure determination

Prior to data collection, crystals were harvested for one minute in 1.8 M NaH_2PO_4/K_2HPO_4, 2% MPD (pH 7.25) and 1% (v/v) glycerol followed by a five second soak in mother liquor containing 20% glycerol as cryoprotectant. Crystals were cryocooled to −170 °C in a nitrogen gas stream. X-ray diffraction data were collected at beamline 9-1 of the Stanford Synchrotron Radiation Laboratory (SSRL) on a 345 mm MAR Research imaging plate using a monochromatic wavelength of 1.025 Å. Images were integrated and scaled with DENZO and SCALEPACK.[33] The H-2K^b–YEA9 crystals belong to orthorhombic space group $P2_12_12$, as do the VSV8 and SEV9 H-2K^b complexes.[5] The structure was determined by molecular replacement using the high-resolution (1.7 Å) H-2K^b–dEV8 by itself (not the H-2K^b–dEV8 complex with T-cell receptor (TCR))[20] as a search model (RCSB Protein Data Bank code 2CKB) with the program AMoRe in CCP4.[34] The complex was refined with CNS,[35] by iterative cycles of positional refinement dynamics, slow-cooling temperature protocols and manual model adjustment. The model was rebuilt from shake-omit maps[28] and σ_A-weighted $2F_o - F_c$ and $F_o - F_c$ maps[36] using the program O.[37] Progress of the refinement was assessed by R_{free} and by avoiding divergence between R_{cryst} and R_{free}.[38] Analysis of the final model with PROCHECK[39] showed 92.1% of the residues are in the most favored regions of the Ramachandran plot, with none in disallowed regions. The YEA9 structure is similar to an unpublished structure at lower resolution previously determined in our laboratory (PDB access code, 1VAD).[40]

Protein Data Bank accession codes

The coordinates and structure factors for H-2K^b–YEA9 have been deposited in the RCSB Protein Data Bank with accession code 1G7P.

Acknowledgments

We thank the staff at SSRL beamline 9-1, S. Greasley, A. Heine, for assistance in data collection, J. Speir and C. Cantu for helpful discussions, N. Tsipouras for preparation of peptides and M. Plebanski and R. Stefanko for excellent technical assistance. Supported by NIH grants CA58896 (I.A.W.) and DK55037 (L.T.), National Health and Medical Research Council of Australia CJ Martin Fellowship (V.A.) and The Austin Research Institute (V.A. and I.F.C.M.). This is publication 14587-MB from the Scripps Research Institute.

References

1. Bjorkman, P. J., Saper, M. A., Samraoui, B., Bennett, W. S., Strominger, J. L. & Wiley, D. C. (1987). Structure of the human class I histocompatibility antigen, HLA-A2. *Nature*, **329**, 506–512.
2. Matsumura, M., Fremont, D. H., Peterson, P. A. & Wilson, I. A. (1992). Emerging principles for the recognition of peptide antigens by MHC class I molecules. *Science*, **257**, 927–934.
3. Madden, D. R., Gorga, J. C., Strominger, J. L. & Wiley, D. C. (1992). The three-dimensional structure of HLA-B27 at 2.1 Å resolution suggests a general mechanism for tight peptide binding to MHC. *Cell*, **70**, 1035–1048.
4. Zhang, W., Young, A. C., Imarai, M., Nathenson, S. G. & Sacchettini, J. C. (1992). Crystal structure of the major histocompatibility complex class I H-2K^b molecule containing a single viral peptide: implications for peptide binding and T-cell receptor recognition. *Proc. Natl Acad. Sci. USA*, **89**, 8403–8407.
5. Fremont, D. H., Matsumura, M., Stura, E. A., Peterson, P. A. & Wilson, I. A. (1992). Crystal structures of two viral peptides in complex with murine MHC class I H-2K^b. *Science*, **257**, 919–927.
6. Rammensee, H. G., Friede, T. & Stevanovic, S. (1995). MHC ligand and peptide motifs: first listing. *Immunogenetics*, **41**, 178–228.
7. Falk, K., Rotzschke, O., Stevanovic, S., Jung, G. & Rammensee, H. G. (1991). Allele-specific motifs

revealed by sequencing of self-peptides eluted from MHC molecules. *Nature*, **351**, 290–296.
8. Saper, M. A., Bjorkman, P. J. & Wiley, D. C. (1991). Refined structure of the human histocompatibility antigen HLA-A2 at 2.6 Å resolution. *J. Mol. Biol.* **219**, 277–319.
9. Apostolopoulos, V., Karanikas, V., Haurum, J. S. & McKenzie, I. F. (1997). Induction of HLA-A2-restricted CTLs to the mucin 1 human breast cancer antigen. *J. Immunol.* **159**, 5211–5218.
10. Daser, A., Urlaub, H. & Henklein, P. (1994). HLA-B27 binding peptides derived from the 57 kD heat shock protein of *Chlamydia trachomatis*: novel insights into the peptide binding rules. *Mol. Immunol.* **31**, 331–336.
11. Mandelboim, O., Bar-Haim, E., Vadai, E., Fridkin, M. & Eisenbach, L. (1997). Identification of shared tumor-associated antigen peptides between two spontaneous lung carcinomas. *J. Immunol.* **159**, 6030–6036.
12. Apostolopoulos, V., Haurum, J. S. & McKenzie, I. F. (1997). MUC1 peptide epitopes associated with five different H-2 class I molecules. *Eur. J. Immunol.* **27**, 2579–2587.
13. Apostolopoulos, V., Pietersz, G. A. & McKenzie, I. F. (1999). MUC1 and breast cancer. *Curr. Opin. Mol. Ther.* **1**, 98–103.
14. Apostolopoulos, V., Pietersz, G. A. & McKenzie, I. F. (2000). Studies of MUC1 peptides. In *Peptide Based Cancer Vaccines* (Kast, M., ed.), pp. 106–120, Landes Bioscience, Chapman and Hall, London. Chapter 7.
15. Apostolopoulos, V., Minmin, Y., Corper, A. L., Wenjun, L., Pietersz, G. A., Plebanski, M. *et al.* (2002). Crystal structure of a non-canonical low affinity peptide complexed with MHC class I: a new approach for vaccine design. *J. Mol. Biol.* **318**, 1293–1305.
16. Gao, L., Walter, J., Travers, P., Stauss, H. & Chain, B. M. (1995). Tumor-associated E6 protein of human papillomavirus type 16 contains an unusual H-2K^b-restricted cytotoxic T cell epitope. *J. Immunol.* **155**, 5519–5526.
17. Fremont, D. H., Stura, E. A., Matsumura, M., Peterson, P. A. & Wilson, I. A. (1995). Crystal structure of an H-2K^b-ovalbumin peptide complex reveals the interplay of primary and secondary anchor positions in the major histocompatibility complex binding groove. *Proc. Natl Acad. Sci. USA*, **92**, 2479–2483.
18. Jackson, M. R., Song, E. S., Yang, Y. & Peterson, P. A. (1992). Empty and peptide-containing conformers of class I major histocompatibility complex molecules expressed in *Drosophila melanogaster* cells. *Proc. Natl Acad. Sci. USA*, **89**, 12117–12121.
19. Matsumura, M., Saito, Y., Jackson, M. R., Song, E. S. & Peterson, P. A. (1992). *In vitro* peptide binding to soluble empty class I major histocompatibility complex molecules isolated from transfected *Drosophila melanogaster* cells. *J. Biol. Chem.* **267**, 23589–23595.
20. Garcia, K. C., Degano, M., Pease, L. R., Huang, M., Peterson, P. A., Teyton, L. *et al.* (1998). Structural basis of plasticity in T cell receptor recognition of a self peptide–MHC antigen. *Science*, **279**, 1166–1172.
21. Degano, M., Garcia, K. C., Apostolopoulos, V., Rudolph, M. G., Teyton, L. & Wilson, I. A. (2000). A functional hot spot for antigen recognition in a superagonist TCR/MHC complex. *Immunity*, **12**, 251–261.
22. Apostolopoulos, V., Chelvanayagam, G., Xing, P. X. & McKenzie, I. F. (1998). Anti-MUC1 antibodies react directly with MUC1 peptides presented by class I H2 and HLA molecules. *J. Immunol.* **161**, 767–775.
23. Speir, J. A., Garcia, K. C., Brunmark, A., Degano, M., Peterson, P. A., Teyton, L. *et al.* (1998). Structural basis of 2C TCR allorecognition of H-2L^d peptide complexes. *Immunity*, **8**, 553–562.
24. Young, A. C., Zhang, W., Sacchettini, J. C. & Nathenson, S. G. (1994). The three-dimensional structure of H-2D^b at 2.4 Å resolution: implications for antigen-determinant selection. *Cell*, **76**, 39–50.
25. Balendiran, G. K., Solheim, J. C., Young, A. C., Hansen, T. H., Nathenson, S. G. & Sacchettini, J. C. (1997). The three-dimensional structure of an H-2L^d-peptide complex explains the unique interaction of L^d with beta-2 microglobulin and peptide. *Proc. Natl Acad. Sci. USA*, **94**, 6880–6885.
26. Molano, A., Erdjument-Bromage, H., Fremont, D. H., Messaoudi, I., Tempst, P. & Nikolic-Zugic, J. (1998). Peptide selection by an MHC H-2K^b class I molecule devoid of the central anchor ("C") pocket. *J. Immunol.* **160**, 2815–2823.
27. Madden, D. R., Garboczi, D. N. & Wiley, D. C. (1993). The antigenic identity of peptide–MHC complexes: a comparison of the conformations of five viral peptides presented by HLA-A2. *Cell*, **75**, 693–708.
28. McRee, D. E. (1993). *Practical Protein Crystallography*, Academic Press, San Diego.
29. Rudolph, M. G., Speir, J. A., Brunmark, A., Mattsson, N., Jackson, M. R., Peterson, P. A. *et al.* (2001). The crystal structures of K^{bm1} and K^{bm8} reveal that subtle changes in the peptide environment impact thermostability and alloreactivity. *Immunity*, **14**, 231–242.
30. Glithero, A., Tormo, J., Haurum, J. S., Arsequell, G., Valencia, G., Edwards, J. *et al.* (1999). Crystal structures of two H-2D^b/glycopeptide complexes suggest a molecular basis for CTL cross-reactivity. *Immunity*, **10**, 63–74.
31. Saito, Y., Peterson, P. A. & Matsumura, M. (1993). Quantitation of peptide anchor residue contributions to class I major histocompatibility complex molecule binding. *J. Biol. Chem.* **268**, 21309–21317.
32. Stura, E. A., Matsumura, M., Fremont, D. H., Saito, Y., Peterson, P. A. & Wilson, I. A. (1992). Crystallization of murine major histocompatibility complex class I H-2K^b with single peptides. *J. Mol. Biol.* **228**, 975–982.
33. Otwinowski, Z. & Minor, W. (1997). Processing of X-ray diffraction data collected in oscillation mode. *Methods Enzymol.* **276**, 307–326.
34. Navaza, J. (1994). AMoRe: an automated package for molecular replacement. *Acta Crystallog. sect. A*, **50**, 157–163.
35. Brünger, A. T., Adams, P. D., Clore, G. M., DeLano, W. L., Gros, P., Grosse-Kunstleve, R. W. *et al.* (1998). Crystallography & NMR system: a new software suite for macromolecular structure determination. *Acta Crystallog. sect. D*, **54**, 905–921.
36. Read, R. J. (1986). Improved Fourier coefficients for maps using phases from partial structures with errors. *Acta Crystallog. sect. A*, **42**, 140–159.
37. Jones, T. A., Zou, J. Y., Cowan, S. W. & Kjeldgaard, A. (1991). Improved methods for binding protein models in electron density maps and the location of errors in these models. *Acta Crystallog. sect. A*, **47**, 110–119.
38. Brünger, A. T. (1992). Free *R* value: a novel statistical quantity for assessing the accuracy of crystal structures. *Nature*, **355**, 472–475.

39. Laskowski, R. A., MacArthur, M. W., Moss, D. & Thornton, J. (1993). PROCHECK: a program to check the stereochemical quality of protein structures. *J. Appl. Crystallog.* **26**, 283–291.
40. Fremont, D.H. (1992). Investigations into the structural basis of the immune response: crystal structures of a class I MHC molecule with bound peptide antigens, an antibody Fab fragment, and phospholipase A2. PhD thesis, University of California, San Diego.
41. Kast, W. M., Roux, L., Curren, J., Blom, H. J., Voordouw, A. C., Meloen, R. H. *et al.* (1991). Protection against lethal Sendai virus infection by *in vivo* priming of virus-specific cytotoxic T lymphocytes with a free synthetic peptide. *Proc. Natl Acad. Sci. USA*, **88**, 2283–2287.
42. Franco, M. A., Lefevre, P., Willems, P., Tosser, G., Lintermanns, P. & Cohen, J. (1994). Identification of cytotoxic T cell epitopes on the VP3 and VP6 rotavirus proteins. *J. Gen. Virol.* **75**, 589–596.
43. Carbone, F. R. & Bevan, M. J. (1989). Induction of ovalbumin-specific cytotoxic T cells by *in vivo* peptide immunization. *J. Expt. Med.* **169**, 603–612.
44. Van Bleek, G. M. & Nathenson, S. G. (1990). Isolation of an endogenously processed immunodominant viral peptide from the class I H-2K^b molecule. *Nature*, **348**, 213–216.
45. Tallquist, M. D., Yun, T. J. & Pease, L. R. (1996). A single T cell receptor recognizes structurally distinct MHC/peptide complexes with high specificity. *J. Expt. Med.* **184**, 1017–1026.
46. Sykulev, Y., Vugmeyster, Y., Brunmark, A., Ploegh, H. L. & Eisen, H. N. (1998). Peptide antagonism and T cell receptor interactions with peptide–MHC complexes. *Immunity*, **9**, 475–483.
47. Udaka, K., Wiesmuller, K. H., Kienle, S., Jung, G. & Walden, P. (1996). Self-MHC-restricted peptides recognized by an alloreactive T lymphocyte clone. *J. Immunol.* **157**, 670–678.
48. Laskowski, R. A. (1995). SURFNET: a program for visualizing molecular surfaces, cavities and intermolecular interactions. *J. Mol. Graph.* **13**, 323–330.

Edited by D. Rees

(Received 20 November 2001; received in revised form 8 March 2002; accepted 9 March 2002)